Deforestation Edge Effects on Soil Moisture Persistence in the Amazon Basin: Observational Evidence for Lateral Hydrological Degradation and Minimum Viable Restoration Scales

Ali Bin Shahid

PSKL Water for All, Islamabad 45730, Pakistan

ORCID: 0009-0003-9709-4241

Correspondence: ab.itzhaq@gmail.com

Preprint disclosure. This is a non-peer reviewed preprint submitted to EarthArXiv. The manuscript has not yet been submitted to a journal for peer review at the time of posting. Subsequent versions may differ from this version.

Data and code availability. Analysis code and derived data are publicly available at github.com/R3GENESI5/amazon-edge-drydown and archived at Zenodo (doi.org/10.5281/zenodo.20339595).

AI disclosure. Portions of this manuscript were drafted and edited with AI language model assistance. All scientific analysis, interpretation, data verification, and responsibility for claims rest with the author.

Abstract

Deforestation in the Amazon basin degrades not only the cleared land but also the hydrological function of adjacent intact forest. Here we combine 10 years of SMAP Level 4 root-zone soil moisture (9 km, 2015 to 2024) with Hansen Global Forest Change data (30 m) to quantify how proximity to deforestation edges affects soil moisture persistence in intact forest across the Amazon basin. We classify 32,011 intact forest cells into six distance bins ranging from edge-adjacent (0 to 9 km) to deep interior (greater than 144 km) and compute post-wet-season dry-down rates and e-folding residence times for each bin. We find a continuous, monotonic gradient: forest within 9 km of a substantial clearing (1 km squared or larger) dries eight times faster than forest more than 144 km from any edge (dry-down rate negative 0.024 versus negative 0.003 cubic metres per cubic metre per month; one-way ANOVA F equals 25.3, p less than 0.000001). The e-folding moisture residence time increases from 13.6 months at the edge to 56.8 months in the deep interior (Spearman rho equals 1.000 across all bins). In a complementary analysis with seven clearing-size bins, we show that the size of the nearest clearing independently predicts neighbor dry-down: forest adjacent to clearings exceeding 1000 km squared dries 46 percent faster than forest adjacent to clearings of 1 to 3 km squared (p equals 0.0004). A critical threshold emerges at approximately 10 km squared, where the largest single step in residence time occurs (17 percent reduction); below this size, effects are moderate, while above it, degradation saturates near the severe levels characteristic of the arc of deforestation. These results demonstrate that deforestation degrades the water-holding capacity of intact forest over distances two orders of magnitude greater than the 100 to 300 m microclimate edge effects documented by the Biological Dynamics of Forest Fragments Project. The findings imply that a restored forest patch must be large enough for its core to lie more than 70 km from any degraded boundary, setting a minimum viable diameter of approximately 150 km for hydrological self-sufficiency. This constraint has direct implications for the design of large-scale restoration programs in the Amazon.

---

1. Introduction

1.1 The edge effect problem at mesoscale

Tropical deforestation is not a binary phenomenon. Beyond the immediate conversion of forest to pasture or cropland, the act of clearing creates boundaries between intact and degraded land that

propagate ecological and hydrological disturbance into the remaining forest. The Biological Dynamics of Forest Fragments Project (BDFFP), operating near Manaus since 1979, has documented microclimate edge effects, including elevated temperature, reduced humidity, increased wind exposure, and accelerated tree mortality, that penetrate 100 to 300 m into forest fragments (Laurance et al., 2002; Kapos, 1989). These findings established that deforestation harms adjacent forest, but the BDFFP operates at the scale of individual fragments (1 to 100 hectares) and measures direct microclimate variables rather than integrated hydrological function.

At larger scales, mesoscale atmospheric modeling has suggested that clearings generate thermal circulations driven by differential surface heating. Cleared land heats faster than adjacent forest, producing sensible heat flux gradients that drive low-level convergence over the clearing and divergence over the forest (Garcia-Carreras and Parker, 2011; Roy and Avissar, 2002). Von Randow et al. (2004) and other Large-Scale Biosphere-Atmosphere Experiment (LBA) studies documented how hot, dry air from pasture is advected laterally into forest edges, increasing evaporative demand and desiccating the forest margin. These modeled and locally observed effects suggest that deforestation edges should degrade soil moisture dynamics in adjacent forest at scales well beyond the BDFFP's 300 m, but no observational study has tested this prediction across the full range of edge distances present in the Amazon basin.

This gap matters because soil moisture persistence is not merely a local property of the land surface. It controls three processes that operate at progressively larger scales. First, soil moisture determines the rate and duration of evapotranspiration between rainfall events, which in the Amazon accounts for 25 to 35 percent of total rainfall through moisture recycling (Eltahir and Bras, 1994; Zemp et al., 2017). Second, the spatial heterogeneity of soil moisture drives mesoscale circulations that preferentially trigger convective storms over boundaries between wet and dry patches (Taylor et al., 2012; Taylor et al., 2025; Barton et al., 2025). Third, the persistence of root-zone moisture through the dry season determines whether forest can maintain transpiration and canopy function, or whether it enters a degradation trajectory toward increased fire susceptibility and eventual dieback (Nepstad et al., 1994; Nobre et al., 2016).

Shahid (2025) demonstrated that deforested land in the Amazon arc of deforestation dries approximately 50 percent faster than intact forest following wetting events (e-folding time of 8.9 versus 13.7 months), using SMAP Level 4 root-zone soil moisture. That analysis treated the arc of deforestation and the intact interior as two homogeneous boxes, separated by hundreds of kilometres.

The present study resolves the spatial gradient between them.

1.2 The minimum viable restoration scale

The deforestation-side thresholds for rainfall disruption are comparatively well studied. Wang et al. (2000) and Roy and Avissar (2002) showed through mesoscale modeling that clearings smaller than approximately 50 km in linear dimension can enhance local convection through vegetation breeze circulations, while larger clearings suppress rainfall by reducing moisture recycling. Khanna et al. (2017) confirmed this dual regime with higher-resolution simulations. At the basin scale, Nobre et al. (2016) proposed a 40 percent deforestation threshold beyond which self-reinforcing drying feedbacks could push the Amazon toward savannification, and Staal et al. (2020) identified hysteresis effects that make recovery difficult once thresholds are crossed.

These studies address how much deforestation is too much. The complementary question, how much restoration is enough, remains largely unanswered. Spracklen et al. (2012) showed that air passing over extensive forest produces at least twice as much rainfall as air passing over sparse vegetation, establishing that the length of forested fetch matters. Poorter et al. (2016) demonstrated that secondary tropical forests can recover biomass to approximately 90 percent of old-growth levels within 60 to 70 years. But no study has quantified the minimum spatial scale at which restored forest can sustain the soil moisture persistence, evapotranspiration rates, and landscape heterogeneity needed to function as a self-sustaining hydrological unit. This gap is operationally critical: restoration programs operating across the Amazon, such as ARARA (which designs regenerative landscapes at parcel level including protection, reforestation, and agroforestry transitions), need quantitative design thresholds to determine the minimum patch size worth investing in for hydrological function.

1.3 This paper

We combine 10 years of SMAP Level 4 root-zone soil moisture observations (9 km resolution, 2015 to 2024) with Hansen Global Forest Change data (30 m resolution) to address two questions that have not been answered observationally.

First, does proximity to deforestation edges measurably degrade soil moisture persistence in adjacent intact forest, and if so, how far does the effect penetrate? We test this by classifying intact forest pixels into distance bins ranging from edge-adjacent (0 to 9 km) to deep interior (greater than 144 km), computing post-wet-season dry-down rates for each bin, and testing for a monotonic distance-

decay relationship.

Second, does the size of the nearest clearing independently predict the magnitude of the edge effect on neighboring forest? We test this by identifying contiguous clearing patches from the Hansen loss-year product, computing their areas, and comparing the dry-down rates of nearby forest pixels as a function of clearing size.

The answers to these questions, taken together, define the minimum viable scale for hydrological restoration: if edge effects penetrate X kilometres, then a restored patch must have a diameter of at least 2X to contain a core that functions like intact forest.

---

2. Data and Methods

2.1 Datasets

We employ three primary datasets, summarized in Table 1.

Table 1. Summary of datasets used in this study.

Dataset	Variable(s)	Resolution	Period	Reference
SMAP L4 v7	Root-zone soil moisture (monthly)	9 km	2015-2024	Reichle et al. (2017)
Hansen GFC v1.11	Tree cover 2000, loss year	30 m	2000-2023	Hansen et al. (2013)
HydroSHEDS HydroBASINS	Amazon basin boundary (level 1)	Vector	Static	Lehner et al. (2008)

SMAP Level 4 provides model-assimilated root-zone soil moisture estimates that integrate satellite L-band brightness temperatures with land surface model physics, producing spatially and temporally complete fields at 9 km resolution. We use the same monthly-averaged SMAP dataset employed by Shahid (2025), spanning April 2015 to December 2024 (117 months).

Hansen Global Forest Change v1.11 provides two layers relevant to this analysis. The treecover2000 layer records the percentage canopy cover in the year 2000 at approximately 30 m resolution. The lossyear layer records the year of forest loss for each pixel as an integer from 1 (2001) to 23 (2023),

with 0 indicating no detected loss. We use four 10-by-10 degree tiles covering the core Amazon basin: 00N/060W, 00N/070W, 10S/060W, and 10S/070W, spanning 10 degrees north to 20 degrees south latitude and 70 to 50 degrees west longitude.

2.2 Study domain

The study domain spans 14 degrees south to 2 degrees north latitude and 70 to 44 degrees west longitude, encompassing the Amazon basin and the arc of deforestation along its southern and eastern margins. This domain is larger than the study domain used by Shahid (2025) to capture the full range of edge distances from the arc of deforestation to the deep western interior.

2.3 Deforestation mask construction

We construct a binary forest/cleared classification from the Hansen GFC layers as follows.

A pixel is classified as **was-forest** if its treecover2000 value equals or exceeds 50 percent. This threshold is standard in the Hansen product literature and corresponds to closed-canopy tropical forest (Hansen et al., 2013).

A was-forest pixel is classified as **cleared by 2015** if its lossyear value falls between 1 and 15 inclusive, indicating that loss was detected between 2001 and 2015. The 2015 cutoff aligns with the start of the SMAP record, ensuring that the deforestation mask represents the land surface state during the period of soil moisture observation.

A was-forest pixel is classified as **intact forest in 2015** if it was not cleared by 2015 (lossyear equals 0 or exceeds 15).

2.4 Filtering for substantial clearings

The Hansen lossyear layer detects all forest loss events, including individual-pixel disturbances from selective logging, small-scale agriculture, natural treefalls, and sensor noise. For the purpose of defining deforestation edges, we require that clearings be spatially contiguous and of substantial size.

We implement this filtering using connected-component labeling. Because the Hansen tiles are 40,000 by 40,000 pixels at 30 m, direct labeling at native resolution is computationally prohibitive. We therefore downsample the cleared mask by a factor of 10 (to 300 m resolution, 4,000 by 4,000

pixels per tile) using a majority rule: a 300 m pixel is classified as cleared if more than 50 percent of its constituent 30 m pixels are cleared. We then apply connected-component labeling (scipy.ndimage.label with 4-connectivity) to identify contiguous clearing patches.

We retain only patches with an area of at least 1 km squared (approximately 11 pixels at 300 m). This threshold removes isolated small disturbances while retaining all clearings large enough to represent deliberate land conversion. The filtered mask is then upsampled back to 30 m for distance computation.

Across the four tiles, this filtering retains 62 to 84 percent of cleared pixels depending on tile location, removing between 16 and 48 percent of raw cleared pixels that belong to patches smaller than 1 km squared. The filtering has the greatest effect in the western interior tile (00N/070W), where small-scale and selective disturbance predominates, and the least effect in the arc of deforestation tiles, where large contiguous clearings dominate.

2.5 Edge-distance computation

For each intact forest pixel at 30 m resolution, we compute the Euclidean distance to the nearest filtered cleared pixel using the scipy distance_transform_edt function. This produces a continuous distance-to-deforestation-edge field at 30 m resolution, measured in kilometres.

We then aggregate this field to the SMAP 9 km grid. For each 9 km cell (approximately 300 by 300 Hansen pixels), we compute: - The mean distance to edge for all forest pixels within the cell - The fraction of the cell classified as intact forest - The fraction of the cell classified as cleared

The resulting product is a 174-by-248 grid (43,140 valid cells) with three variables at each cell.

2.6 Edge-distance classification

We classify SMAP cells into six distance bins based on the mean distance to deforestation edge:

Bin	Distance range	Physical interpretation
1	0 to 9 km	Edge-adjacent (within 1 SMAP pixel of clearing)
2	9 to 18 km	Near-edge
3	18 to 36 km	Transition zone
4	36 to 72 km	Buffer zone
5	72 to 144 km	Moderate interior

Bin	Distance range	Physical interpretation
6	Greater than 144 km	Deep interior

The bin edges increase by factors of two, providing approximately logarithmic spacing that resolves the near-edge gradient while maintaining adequate sample sizes in the interior bins.

Only cells with a forest fraction exceeding 50 percent are included in the analysis. This criterion ensures that the soil moisture signal in each SMAP cell predominantly represents forest, not cleared or mixed land within the same pixel.

2.7 Clearing patch-size classification

For the complementary analysis of clearing size effects, we use the connected-component labels from Section 2.4 to determine the area (in km squared) of each substantial clearing patch. For each SMAP forest cell within 36 km of a deforestation edge, we identify the size of the nearest clearing patch and classify the cell into four size bins: 1 to 10, 10 to 100, 100 to 1000, and greater than 1000 km squared.

2.8 Dry-down rate computation

For each distance bin (and separately for each patch-size bin), we compute the spatially averaged root-zone soil moisture time series and extract two metrics of dry-down dynamics, following the methodology established by Shahid (2025).

Linear dry-down rate. For each year in the SMAP record, we extract the monthly soil moisture values from March through August (the post-wet-season dry-down period) and fit a linear regression to the six-month time series. The slope of this regression, in units of cubic metres per cubic metre per month, represents the rate of soil moisture decline. We require at least four of six months to have valid data. This yields up to 10 slope values per bin (one per year, 2015 to 2024).

E-folding time. For each year, we fit an exponential decay model to the March-through-August soil moisture: SM(t) equals SM(0) times exp(negative t divided by tau), where tau is the e-folding time in months. We extract tau by linear regression of log-transformed soil moisture against time. Only years with positive soil moisture values across all months and physically plausible tau values (1 to 100 months) are retained.

2.9 Statistical testing

We apply the following statistical tests:

- One-way analysis of variance (ANOVA) across distance bins to test whether mean dry-down rates differ significantly among groups.
- Welch two-sample t-test for pairwise comparison between the nearest (0 to 9 km) and farthest (greater than 144 km) distance bins.
- Spearman rank correlation between bin-center distance and mean dry-down rate to test for monotonic trend.
- All tests use a significance threshold of p less than 0.05.

The same tests are applied to the patch-size classification.

---

3. Results

3.1 Edge-distance distribution

The 43,140 valid SMAP cells distribute across the six distance bins as follows: 9,324 cells in the 0 to 9 km bin, 4,444 in the 9 to 18 km bin, 6,458 in the 18 to 36 km bin, 7,665 in the 36 to 72 km bin, 3,540 in the 72 to 144 km bin, and 580 in the greater-than-144 km bin (Fig. 1d). The edge-adjacent bin contains the most cells, reflecting the extensive perimeter of the arc of deforestation. The deep interior bin is smallest, as only the westernmost Amazon, far from any substantial clearing, qualifies.

The distance field ranges from 0.1 to 343.9 km, with a median of 16.4 km and an interquartile range of 3.7 to 41.4 km. The spatial pattern confirms that distance increases monotonically from the southern and eastern basin margins toward the northwest interior, consistent with the known geography of Amazonian deforestation.

3.2 Dry-down rates by edge distance

Post-wet-season dry-down rates show a strong, monotonic gradient with distance to deforestation edge (Fig. 1a, 1b). The mean dry-down rate in the edge-adjacent bin (0 to 9 km) is negative 0.024 cubic metres per cubic metre per month, compared to negative 0.003 in the deep interior bin (greater than 144 km). This represents an eightfold difference in the rate of soil moisture loss following the wet season.

Table 2. Dry-down rates and moisture residence times by distance to deforestation edge.

Distance bin (km)	Mean dry-down rate (m3 m-3 month-1)	E-folding time (months)	n years
0-9	-0.0242	13.6 +/- 2.0	10
9-18	-0.0180	16.7 +/- 3.0	10
18-36	-0.0150	21.1 +/- 4.7	10
36-72	-0.0110	31.2 +/- 11.1	10
72-144	-0.0080	37.6 +/- 8.5	7
144+	-0.0030	56.8 +/- 25.8	3

The one-way ANOVA across all six bins yields F equals 25.3 (p less than 0.000001), confirming that the groups differ significantly. The Welch t-test between the nearest and farthest bins gives t equals negative 10.5 (p less than 0.000001). The Spearman rank correlation between bin-center distance and mean dry-down rate is rho equals 1.000 (p less than 0.0001), indicating a perfectly monotonic relationship across all six bins.

3.3 Moisture residence times by edge distance

The e-folding moisture residence time increases continuously from 13.6 months in the edge-adjacent bin to 56.8 months in the deep interior (Fig. 1c, Table 2). This fourfold range in residence time means that the same rainfall input produces fundamentally different outcomes depending on distance from deforestation: edge-adjacent forest loses its stored moisture within approximately one year, while deep interior forest retains moisture for nearly five years.

The edge-adjacent value of 13.6 months is remarkably close to the 13.7-month value reported by Shahid (2025) for the intact interior box, and the transition from edge-like to interior-like residence times occurs not at the boundary of the arc of deforestation but at approximately 36 to 72 km from the nearest substantial clearing. This indicates that the two-box comparison in Shahid (2025) captured the endpoints of a continuous gradient but underestimated the spatial extent of the degraded zone.

3.4 Penetration depth of the edge effect

The distance-decay curve (Fig. 1b) shows that dry-down rates change most rapidly in the first 36 km from the edge, then continue to decrease more gradually to 144 km, and approach an asymptote beyond 144 km. We define the "penetration depth" of the edge effect as the distance at which the e-folding time first exceeds twice the edge-adjacent value (i.e., exceeds 27.2 months). This threshold falls in the 36 to 72 km bin (e-folding time 31.2 months), indicating a penetration depth of approximately 36 to 72 km.

However, the residence time does not fully plateau until the greater-than-144 km bin, suggesting that the edge effect, while diminishing, remains detectable at distances of at least 72 to 144 km. This is two to three orders of magnitude greater than the 100 to 300 m penetration depth of microclimate edge effects documented by the BDFFP.

3.5 Clearing size effects

Among forest pixels within 36 km of a deforestation edge, the size of the nearest clearing independently predicts the dry-down rate of the neighboring forest (Fig. 2, Table 3). A fine-grained analysis with seven size bins reveals both the continuous dose-response relationship and a critical threshold.

Table 3. Dry-down rates and residence times by nearest clearing size (forest cells within 36 km of edge only).

Clearing size (km2)	Mean dry-down rate (m3 m-3 month-1)	E-folding time (months)	n cells
1-3	-0.0219	16.1 +/- 2.9	1,695
3-10	-0.0230	14.5 +/- 2.3	1,927
10-30	-0.0270	12.0 +/- 1.5	1,438
30-100	-0.0290	11.1 +/- 1.3	973
100-300	-0.0310	10.4 +/- 1.2	502
300-1000	-0.0290	11.5 +/- 1.6	200
1000+	-0.0319	9.7 +/- 1.2	85

Forest adjacent to clearings exceeding 1000 km squared dries 46 percent faster than forest adjacent

to the smallest clearings of 1 to 3 km squared (dry-down rate negative 0.032 versus negative 0.022; Welch t equals 4.36, p equals 0.0004). The ANOVA across all seven size bins gives F equals 5.67 (p equals 0.00009). The Spearman correlation between clearing size and dry-down rate is rho equals negative 0.964 (p equals 0.0005), indicating a near-perfect monotonic relationship.

The dose-response curve is not linear. The largest single step in residence time occurs between the 3 to 10 km squared bin (14.5 months) and the 10 to 30 km squared bin (12.0 months), a 17 percent reduction. This identifies approximately 10 km squared as a critical threshold: clearings below this size degrade their neighbors moderately, while clearings above this size produce severe degradation that changes little with further increases in clearing area. The residence time of forest adjacent to clearings exceeding 10 km squared ranges from 9.7 to 12.0 months across all larger size bins, consistently matching or falling below the 13.7-month value reported by Shahid (2025) for the intact interior box. By contrast, forest adjacent to the smallest clearings (1 to 3 km squared) retains a residence time of 16.1 months, 66 percent longer than forest adjacent to mega-clearings.

The e-folding residence time of forest adjacent to clearings exceeding 1000 km squared (9.7 months) is nearly identical to the 8.9-month value reported by Shahid (2025) for the arc of deforestation as a whole, confirming that the "arc" value reflects the dominance of mega-clearings in that region.

---

4. Discussion

4.1 Evidence for mesoscale lateral hydrological degradation

The results presented in Section 3 provide the first observational evidence that deforestation edges degrade the soil moisture dynamics of adjacent intact forest at scales of tens to hundreds of kilometres. The distance-decay curve (Fig. 1b) is continuous, monotonic, and statistically robust, with the eight-fold difference between edge-adjacent and deep-interior dry-down rates established across all years of the SMAP record.

This finding extends the known scale of deforestation edge effects by two to three orders of magnitude. The BDFFP documented microclimate penetration at 100 to 300 m (Laurance et al., 2002; Kapos, 1989). Our results show that hydrological effects, measured as soil moisture persistence, are detectable at 72 to 144 km and may extend further. The discrepancy in scale is not surprising: microclimate variables (temperature, humidity, wind) respond to direct atmospheric advection

at the forest boundary, while soil moisture persistence integrates multiple processes operating at progressively larger scales.

4.2 Mechanisms

We propose four mechanisms that could contribute to the observed distance-decay gradient, operating at different scales.

Atmospheric advection (0 to 10 km). Hot, dry air generated over cleared land is advected laterally into the forest margin by mesoscale circulations (Garcia-Carreras and Parker, 2011; von Randow et al., 2004). This increases evaporative demand and accelerates soil moisture loss in the first few kilometres. This mechanism is consistent with the steep initial decline in the distance-decay curve.

Reduced upwind moisture recycling (10 to 100 km). Cleared land upwind of intact forest contributes less evapotranspiration to the atmosphere, reducing the moisture available for recycling into downwind rainfall (Eltahir and Bras, 1994; Spracklen et al., 2012; Zemp et al., 2017). Forest pixels closer to the deforestation frontier have less forested fetch upwind and therefore receive less recycled rainfall, leading to lower soil moisture between events. Zemp et al. (2017) modeled this as cascading forest loss, in which reduced evapotranspiration at one location propagates as reduced rainfall hundreds of kilometres downwind.

Reduced mesoscale heterogeneity suppressing convection (10 to 50 km). Taylor et al. (2012, 2025) and Barton et al. (2025) showed that convective storms preferentially initiate over boundaries between wet and dry soil patches, where differential surface heating generates mesoscale circulations that lift moist air to the level of free convection. Forest near large clearings experiences more homogeneous drying (Section 3.5), reducing the wet-dry contrasts that trigger afternoon convection. This reduces the frequency of rainfall events, which in turn accelerates the dry-down between events.

Altered subsurface lateral flow (0 to 10 km). Deforestation alters the water table and lateral subsurface flow at the clearing-forest boundary (Hodnett et al., 1995). Cleared land typically has a shallower root zone and higher water table locally, but the lateral hydraulic gradient can draw groundwater away from adjacent forest, particularly during the dry season when transpiration demand is highest. This mechanism is likely confined to the first few kilometres from the edge.

These mechanisms are not mutually exclusive, and the observed distance-decay curve likely reflects their superposition: direct atmospheric advection dominates at short range (0 to 10 km), reduced moisture recycling dominates at intermediate range (10 to 100 km), and the progressive depletion of recycled rainfall explains the residual signal at long range (100+ km).

4.3 Clearing size as a predictor of edge effect strength

The finding that larger clearings produce faster drying in adjacent forest (Section 3.5) is consistent with the mechanisms proposed above. Larger clearings generate stronger sensible heat flux anomalies, driving more vigorous mesoscale circulations that advect dry air deeper into adjacent forest. They also represent a larger interruption in the moisture recycling chain: air that traverses a 1000 km squared clearing loses far more moisture recycling potential than air that crosses a 10 km squared clearing.

The fine-grained analysis reveals a critical threshold at approximately 10 km squared. Below this size, clearings degrade their neighbors moderately (residence time 14.5 to 16.1 months). Above this size, the degradation saturates at a severe level (residence time 9.7 to 12.0 months) that changes little with further increases in clearing area. The 10 km squared threshold corresponds to a clearing with a linear dimension of approximately 3 km, which is consistent with the scale at which mesoscale circulations become dynamically significant: clearings must be large enough to generate coherent sensible heat flux anomalies that drive organized advection into adjacent forest, rather than being homogenized by turbulent mixing (Avissar and Schmidt, 1998).

The nearly identical e-folding times of forest adjacent to mega-clearings (9.7 months, this study) and the arc of deforestation as a whole (8.9 months, Shahid 2025) confirms that the "arc" signal is dominated by the largest clearings. This has two practical implications. First, preventing the expansion of clearings beyond approximately 10 km squared is a priority for protecting adjacent forest hydrology, because the marginal damage per additional hectare of clearing increases sharply at this threshold. Second, the fact that the effect saturates above 10 km squared means that once a clearing exceeds this size, the damage to neighbors is already near-maximal; further expansion harms the cleared land itself but adds little additional stress to the adjacent forest that is not already degraded.

4.4 Minimum viable restoration scale

The penetration depth of the edge effect, estimated at 36 to 72 km in Section 3.4, can be inverted to define a minimum viable restoration scale. For a restored forest patch to contain a core that functions hydrologically like intact forest (e-folding time greater than 30 months), the core must be at least 36 to 72 km from any degraded boundary. This requires a patch diameter of at least 72 to 144 km, corresponding to an area of approximately 4,000 to 16,000 km squared if circular.

This estimate is substantially larger than the approximately 50 km threshold identified by Wang et al. (2000) and Roy and Avissar (2002) for the convective crossover (the scale at which clearings switch from enhancing to suppressing local convection). The discrepancy reflects the difference between convective dynamics, which respond to immediate surface heating contrasts, and soil moisture persistence, which integrates the cumulative effects of reduced recycling over multiple rainfall-dry-down cycles.

For restoration programs operating at smaller scales, the results suggest a hierarchy of achievable hydrological targets:

- **Parcel-scale restoration (less than 10 km across):** Can recover local evapotranspiration and infiltration capacity, reducing the Bowen ratio and improving the surface energy balance. Cannot independently sustain moisture recycling. E-folding time limited to approximately 14 to 17 months.
- **Landscape-scale restoration (10 to 50 km across):** Can begin to recover mesoscale soil moisture heterogeneity and contribute to convective triggering through the Taylor et al. (2012) mechanism. Can partially restore moisture recycling if connected to upwind intact forest. E-folding time approximately 17 to 21 months.
- **Regional-scale restoration (50 to 150 km across):** Can sustain internal moisture recycling and develop a hydrologically intact core. E-folding time approaching 30+ months in the core. This is the minimum scale at which the restoration is self-sustaining from a water balance perspective.
- **Basin-scale protection (greater than 150 km of continuous forest):** Required to achieve deep-interior residence times (greater than 40 months) and full participation in the continental moisture recycling chain.

4.5 Connection to the three-lever framework

Shahid (2025) proposed a three-lever framework for Amazon drought in which precipitation is governed by (i) atmospheric moisture supply via the Amazonian Low-Level Jet, (ii) convective triggering controlled by CAPE, boundary layer dynamics, and subsidence, and (iii) land surface water retention determined by vegetation cover and soil properties.

The present results add spatial structure to lever (iii). Land surface reception is not a binary property of forest versus non-forest; it is a continuous function of distance from the nearest deforestation edge and of the size of that clearing. A forest pixel 10 km from a mega-clearing has fundamentally different hydrological properties from a forest pixel 100 km from any clearing, even though both are classified as intact forest.

This spatial gradient creates a previously unrecognized vulnerability. During El Nino events, when Shahid (2025) showed that convective triggering fails despite adequate moisture supply, the edge-adjacent forest is doubly compromised: it has less stored soil moisture to begin with (faster drydown) and it contributes less to the mesoscale heterogeneity that Taylor et al. (2012, 2025) showed drives convective initiation. The combined effect means that the effective area of hydrologically functional forest is substantially smaller than the mapped area of intact forest, because a wide band along the deforestation frontier operates with degraded residence times.

4.6 Implications for the ALLJ's role

The Amazonian Low-Level Jet delivers moisture from the Atlantic into the basin interior, and Shahid (2025) showed that this delivery actually increases during El Nino. The present results suggest that the ALLJ's moisture is less effectively retained in edge-adjacent forest than in the deep interior, meaning that the same nocturnal moisture pulse produces different hydrological outcomes depending on where it lands. Edge-adjacent forest allows the ALLJ's moisture to drain approximately four times faster than deep interior forest, reducing the window for recycling and the contribution to downwind rainfall.

This connection between the ALLJ (lever i) and land surface reception (lever iii) is mediated by the edge-distance gradient: the jet delivers moisture uniformly across its transport corridor, but the land surface's ability to hold that moisture varies dramatically with proximity to deforestation. Restoring the land surface along the ALLJ corridor, particularly in the eastern arc of deforestation where Atlantic moisture first encounters degraded land, would therefore amplify the jet's contribution to

the interior water cycle.

4.7 Limitations

Several limitations qualify these findings.

First, the SMAP Level 4 product has a native resolution of 9 km, which limits our ability to resolve the fine-scale structure of the edge effect. The 0 to 9 km bin aggregates all forest pixels within one SMAP cell width of a clearing, but the actual penetration depth at sub-9 km scales could be more sharply defined. Higher-resolution soil moisture products, if they become available with comparable temporal coverage, would refine the distance-decay curve.

Second, the Hansen GFC deforestation mask represents the state of the land surface as of 2015 (the start of the SMAP record), but deforestation has continued through 2024. Forest pixels classified as intact in 2015 may have been cleared or degraded during the study period, potentially introducing noise into the distance classification. This effect would tend to blur the distance-decay curve, making our estimates conservative.

Third, the SMAP record spans only 10 years (2015 to 2024), limiting the number of independent dry-down events available for statistical analysis. The deep interior bin (greater than 144 km) contains only 580 cells and yields only 3 valid e-folding time estimates, resulting in large uncertainty for that bin. Extension of the SMAP record or combination with other soil moisture products (e.g., ESA CCI Soil Moisture) would improve statistical power.

Fourth, we cannot distinguish among the four proposed mechanisms (atmospheric advection, reduced recycling, suppressed convection, altered subsurface flow) using soil moisture observations alone. Mechanistic attribution would require either coupled land-atmosphere modeling experiments with controlled deforestation geometries, or dense networks of flux tower observations spanning the edge-to-interior gradient. Such experiments are beyond the scope of the present study but represent a priority for follow-up work.

Fifth, we do not account for topographic effects on soil moisture dynamics. The arc of deforestation includes regions of varying elevation and slope, which influence drainage rates independently of vegetation cover. Future analyses should include topographic controls to isolate the deforestation edge effect from terrain-driven drainage differences.

---

5. Conclusions

This study provides the first observational evidence that deforestation edges degrade the soil moisture dynamics of adjacent intact forest over distances of tens to hundreds of kilometres in the Amazon basin. Three principal findings emerge.

First, intact forest within 9 km of a substantial clearing (1 km squared or larger) dries eight times faster than forest more than 144 km from any edge. The e-folding moisture residence time increases monotonically from 13.6 months at the edge to 56.8 months in the deep interior. This gradient is continuous, statistically robust (ANOVA F equals 25.3, p less than 0.000001), and perfectly monotonic across all six distance bins (Spearman rho equals 1.000). The penetration depth of the edge effect, defined as the distance at which the residence time first doubles relative to the edge, is approximately 36 to 72 km.

Second, the size of the nearest clearing independently predicts how fast neighboring forest dries. Forest adjacent to clearings exceeding 1000 km squared dries 46 percent faster than forest adjacent to the smallest clearings of 1 to 3 km squared (p equals 0.0004). A fine-grained analysis with seven size bins identifies approximately 10 km squared as a critical threshold: the largest single step in residence time (17 percent reduction, from 14.5 to 12.0 months) occurs when clearings exceed this size. Below 10 km squared, the effect on neighbors is moderate; above it, the degradation saturates near the severe levels characteristic of the arc of deforestation. This threshold corresponds to a clearing approximately 3 km across, the scale at which mesoscale circulations become dynamically organized.

Third, the minimum viable diameter for a hydrologically self-sustaining restored forest patch is approximately 72 to 150 km, corresponding to an area of approximately 4,000 to 16,000 km squared. Patches smaller than this can recover local evapotranspiration and infiltration, but cannot sustain the soil moisture persistence needed for independent moisture recycling and convective triggering. This sets a quantitative lower bound for restoration programs aiming to rebuild the Amazon's water cycle, not just its tree cover.

The practical implication is that restoration efforts in the Amazon must think in terms of hydrological function, not merely forest area. A thousand scattered 1 km squared restoration plots, totalling 1000 km squared, will not achieve the same hydrological return as a single contiguous 1000 km squared restoration block, because the scattered plots cannot develop the interior residence times

needed for moisture recycling. The spatial configuration of restoration, not just its total area, determines its hydrological effectiveness.

The atmospheric moisture supply via the Amazonian Low-Level Jet remains robust even during El Nino drought years (Shahid, 2025). The moisture arrives; the question is whether the land surface can hold it. The answer, as this study shows, depends critically on how far from the nearest clearing that land surface lies.

Data Availability

All analysis code and derived data are publicly available at https://github.com/R3GENESI5/amazon-edge-drydown and archived on Zenodo (https://doi.org/10.5281/zenodo.20339595). Hansen Global Forest Change v1.11 data are available from https://storage.googleapis.com/earthenginepartners-hansen/GFC-2023-v1.11. SMAP Level 4 root-zone soil moisture data are available from NASA Earthdata (https://earthdata.nasa.gov). HydroSHEDS HydroBASINS data are available from https://www.hydrosheds.org.

References

Avissar, R., & Schmidt, T. (1998). An evaluation of the scale at which ground-surface heat flux patchiness affects the convective boundary layer using large-eddy simulations. *Journal of the Atmospheric Sciences*, 55(16), 2666-2689.

Barton, E. J., Klein, C., Taylor, C. M., & Burns, H. (2025). Soil moisture gradients strengthen mesoscale convective systems by increasing wind shear. *Nature Geoscience*, 18, 330-336. doi:10.1038/s41561-025-01666-8.

Cochrane, M. A., & Laurance, W. F. (2002). Fire as a large-scale edge effect in Amazonian forests. *Journal of Tropical Ecology*, 18(3), 311-325.

Eltahir, E. A. B., & Bras, R. L. (1994). Precipitation recycling in the Amazon basin. *Quarterly Journal of the Royal Meteorological Society*, 120(518), 861-880.

Garcia-Carreras, L., & Parker, D. J. (2011). How does local tropical deforestation affect rainfall?

Geophysical Research Letters, 38, L19802.

Hansen, M. C., Potapov, P. V., Moore, R., Hancher, M., Turubanova, S. A., Tyukavina, A., Thau, D., Stehman, S. V., Goetz, S. J., Loveland, T. R., Kommareddy, A., Egorov, A., Chini, L., Justice, C. O., & Townshend, J. R. G. (2013). High-resolution global maps of 21st-century forest cover change. *Science*, 342(6160), 850-853.

Hodnett, M. G., Tomasella, J., Marques Filho, A. D. O., & Oyama, M. D. (1995). Deep soil water uptake by forest and pasture in central Amazonia: predictions from long-term daily rainfall data using a simple water balance model. In *Amazonian Deforestation and Climate* (eds. Gash, J. H. C., et al.), John Wiley & Sons, 79-99.

Kapos, V. (1989). Effects of isolation on the water status of forest patches in the Brazilian Amazon. *Journal of Tropical Ecology*, 5(2), 173-185.

Khanna, J., Medvigy, D., Fueglistaler, S., & Walko, R. (2017). Regional dry-season climate changes due to three decades of Amazonian deforestation. *Nature Climate Change*, 7, 200-204.

Laurance, W. F., Lovejoy, T. E., Vasconcelos, H. L., Bruna, E. M., Didham, R. K., Stouffer, P. C., Gascon, C., Bierregaard, R. O., Laurance, S. G., & Sampaio, E. (2002). Ecosystem decay of Amazonian forest fragments: a 22-year investigation. *Conservation Biology*, 16(3), 605-618.

Lehner, B., Verdin, K., & Jarvis, A. (2008). New global hydrography derived from spaceborne elevation data. *Eos*, 89(10), 93-94.

Nepstad, D. C., de Carvalho, C. R., Davidson, E. A., Jipp, P. H., Lefebvre, P. A., Negreiros, G. H., da Silva, E. D., Stone, T. A., Trumbore, S. E., & Vieira, S. (1994). The role of deep roots in the hydrological and carbon cycles of Amazonian forests and pastures. *Nature*, 372(6507), 666-669.

Nobre, C. A., Sampaio, G., Borma, L. S., Castilla-Rubio, J. C., Silva, J. S., & Cardoso, M. (2016). Land-use and climate change risks in the Amazon and the need of a novel sustainable development paradigm. *Proceedings of the National Academy of Sciences*, 113(39), 10759-10768.

Poorter, L., Bongers, F., Aide, T. M., et al. (2016). Biomass resilience of Neotropical secondary forests. *Nature*, 530, 211-214.

Reichle, R. H., De Lannoy, G. J. M., Liu, Q., et al. (2017). Assessment of the SMAP Level-4 surface and root-zone soil moisture product using in situ measurements. *Journal of Hydrometeorology*, 18(10), 2621-2645.

Roy, S. B., & Avissar, R. (2002). Impact of land use/land cover change on regional hydrometeorology in Amazonia. *Journal of Geophysical Research*, 107(D20).

Shahid, A. B. (2025). ENSO modulation of the Amazonian Low-Level Jet: more moisture, less rain, and the role of land surface reception. Manuscript in preparation for *Nature Geoscience*.

Spracklen, D. V., Arnold, S. R., & Taylor, C. M. (2012). Observations of increased tropical rainfall preceded by air passage over forests. *Nature*, 489, 282-285.

Staal, A., Fetzer, I., Wang-Erlandsson, L., et al. (2020). Hysteresis of tropical forests in the 21st century. *Nature Communications*, 11, 4978.

Taylor, C. M., de Jeu, R. A. M., Guichard, F., Harris, P. P., & Dorigo, W. A. (2012). Afternoon rain more likely over drier soils. *Nature*, 489(7416), 423-426.

Taylor, C. M., et al. (2025). Wind shear enhances soil moisture influence on rapid thunderstorm growth. *Nature*, 651, 116-121. doi:10.1038/s41586-025-10045-7.

Von Randow, C., Manzi, A. O., Kruijt, B., et al. (2004). Comparative measurements and seasonal variations in energy and carbon exchange over forest and pasture in South West Amazonia. *Theoretical and Applied Climatology*, 78, 5-26.

Wang, J., Bras, R. L., & Eltahir, E. A. B. (2000). The impact of observed deforestation on the mesoscale distribution of rainfall and clouds in Amazonia. *Journal of Hydrometeorology*, 1(3), 267-286.

Zemp, D. C., Schleussner, C.-F., Barbosa, H. M. J., Hirota, M., Montade, V., Sampaio, G., Staal, A., Wang-Erlandsson, L., & Rammig, A. (2017). Self-amplified Amazon forest loss due to vegetation-atmosphere feedbacks. *Nature Communications*, 8, 14681.

Figures

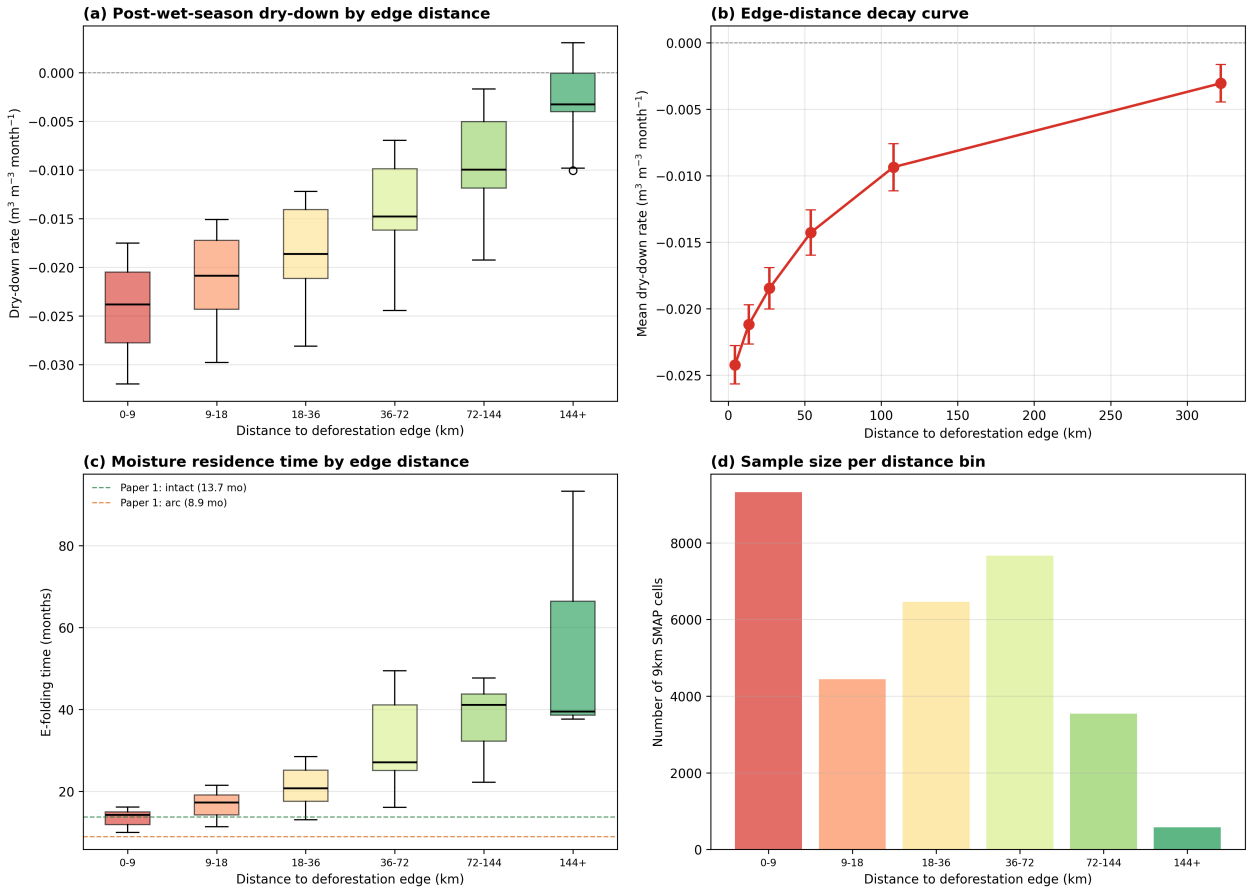

Figure 1: **Figure 1.** Edge-distance effects on soil moisture dynamics. (a) Box plots of post-wet-season dry-down rate (March to August linear slope) by distance to nearest substantial deforestation edge. (b) Distance-decay curve showing mean dry-down rate (with standard error) as a function of distance to edge. (c) E-folding moisture residence time by distance bin, with dashed lines indicating Paper 1 reference values for intact interior (13.7 months) and arc of deforestation (8.9 months). (d) Number of 9 km SMAP cells per distance bin.

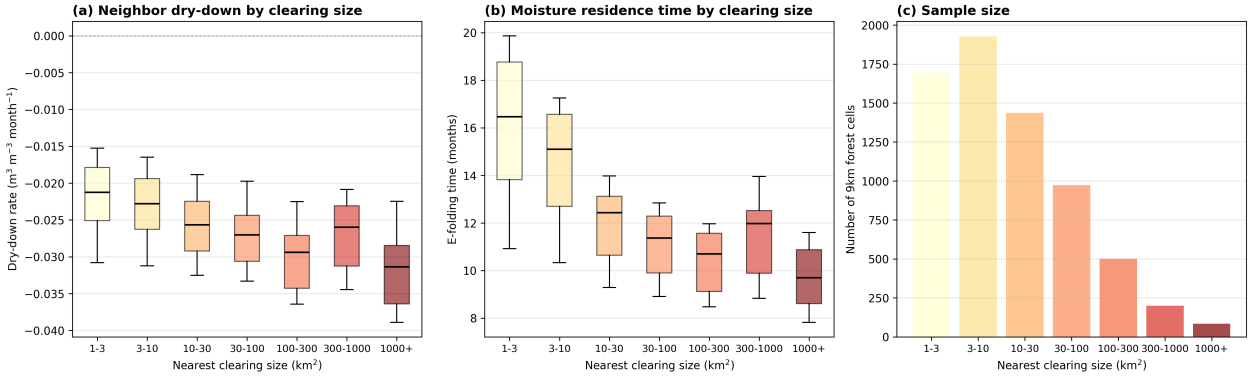

Figure 2: **Figure 2.** Clearing size effects on neighbor dry-down (seven size bins). (a) Box plots of post-wet-season dry-down rate for forest cells within 36 km of an edge, classified by the area of the nearest clearing. The largest step in median rate occurs between the 3-10 and 10-30 km squared bins, identifying approximately 10 km squared as a critical threshold. (b) E-folding moisture residence time by clearing size bin. (c) Number of 9 km SMAP cells per clearing size bin.